Materiales de Construcción
Vol. 74, Issue 353, January-March 2024, e332
ISSN-L: 0465-2746
https://doi.org/10.3989/mc.2024.357623

Ultramarine blue pigment degradation in cementitious materials: a new approach to the phenomenon

G. Rodríguez de Sensale[a,b], S. Chinchón-Payá[c], V. de Lima[a], A. Aguado[d], I. Segura[d] ✉

a. Instituto de la Construcción, Universidad de la República, (Montevideo, Uruguay)
b. Instituto de Ensayo de Materiales, Universidad de la República, (Montevideo, Uruguay)
c. Instituto de Ciencias de la Construcción Eduardo Torroja (IETcc-CSIC), (Madrid, Spain)
d. Departamento de Ingeniería Civil y Ambiental, Universidad Politécnica de Cataluña (Barcelona, Spain)
✉: ignacio.segura@upc.edu

Received 26 June 2023
Accepted 20 November 2023
Available on line 13 March 2024

ABSTRACT: The paper analyses the degradation process of commercial ultramarine blue pigments in cementitious materials. For this purpose, two commercial pigments (with and without a protective coating) in different solutions and cement pastes are studied incrementally. The results show that pigment degradation occurs due to an ion exchange phenomenon; during hydration high ion contents are released, calcium and potassium being the most aggressive for the pigment. Calcium distorts the unit cell; between the sodium of the pigment and the potassium in the medium a cation exchange phenomenon takes place. Both processes lead to the diffusion of sulphate and sulphide ions from the pigment to the medium causing loss of colour and the formation of ettringite.

KEY WORDS: Ultramarine blue pigment; Degradation; Cement; Paste.

Citation/Citar como: Rodríguez de Sensale G, Chinchón-Payá S, de Lima V, Aguado A, Segura I. 2024. Ultramarine blue pigment degradation in cementitious materials: a new approach to the phenomenon. Mater. Construcc. 74(353): e332. https://doi.org/10.3989/mc.2024.357623.

RESUMEN: *Degradación del pigmento azul de ultramar en materiales cementicios: una nueva aproximación al fenómeno.* En el presente artículo se analiza el proceso de degradación del pigmento azul de ultramar en materiales cementicios. Para ello se han estudiado dos pigmentos comerciales (con y sin recubrimiento protector) en diferentes soluciones y pastas de cemento, de manera incremental. Los resultados muestran que la degradación de los pigmentos es debida a un fenómeno de intercambio iónico; durante la hidratación del cemento se liberan altos contenidos de iones, siendo el calcio y el potasio los más agresivos para el pigmento. El calcio distorsiona la celda unitaria del pigmento y entre el sodio del pigmento y el potasio del medio se produce un fenómeno de intercambio catiónico. Ambos procesos conducen a la difusión de iones sulfato y sulfuro desde el pigmento al medio, la degradación del cromóforo con la consiguiente pérdida de color y la formación de etringita.

PALABRAS CLAVE: Pigmento azul ultramar; Degradación; Cemento; Pastas de cemento.

1. INTRODUCTION

The ultramarine blue pigment (UB), that was extensively used in Europe in the 14th and 15th centuries, was first imported to Europe from Asia. The pigment was obtained by the purification of lapis lazuli (a semi-precious stone, from the Latin *lapis*, stone, and *lazulus*, blue) by crushing, grinding and cleaning the raw material to separate the other minerals from lazurite (1). Therefore, the use of UB pigment was limited due to its high price. In 1828, an artificial UB was synthesized by Guimet, who, in 1830, started a factory for the commercial production of the pigment (2); the synthetic pigment was rapidly adopted soon after its invention. A good account of the manufacturing processes and synthesis of UB can be found in the literature (2-5).

In general, UB is a pigment whose fundamental structure is a sodium aluminosilicate type zeolite, with a chromophore structure of polysulphides inside the zeolite cell. In this type of structure, the skeleton is formed by chains of aluminosilicates that join to form a cage-like structure. Sodium ions and chromophores are located inside the cell. Synthetic ultramarine samples have a higher chromophore concentration than natural pigments (5, 6).

UB has a general chemical formula of $A_n((Al, Si)_{12}O_{24})X_2$, where A represents the cations included in the structure (mainly Na^+, although it can also include K^+, Mg^{2+}, Ca^{2+}) and X represents the anions included in the structure, fundamentally SO_4^{2-} and S_3^- (7). These pigments, due to their similarity to zeolites, have a high cation exchange capacity. Therefore, the sodium atoms can be replaced by other cations, among which are K, Ca and Mg. Many studies have been published about the structure of the aluminosilicate framework of natural and synthetics UB (5, 8).

In the world of art and art restoration, the deterioration of ultramarine blue is known as "ultramarine sickness" or "ultramarine disease" (9-14). Different alternatives have been developed for the protection of UB pigment from degradation. Gobeltz et al. (15) investigated the encapsulation of the chromophores into the sodalite structure during the synthesis of the UB pigment and confirmed the results with a source of polysulphides. Liu et al. (16) proposed a two-step silica coating process (sol−gel process followed by dense liquid process used to form silica films on surfaces to minimize photodegradation). Compared with the single-step sol−gel or the dense-liquid-coating process, the two-step process produces magnetic nanocomposites with the highest protection against acid attack at the lowest level of silica coatings with maximized magnetization. Li et al. (17) proposed another two-step method for the preparation of acid-resistant UB particles with highly dense, smooth and uniform silica films. They compared the resistance to hydrochloric acid of the UB prepared with the method with those achieved by dense liquids, sol-gel, and conventional two-step coatings. A great enhancement of acid resistance for ultramarine blue was achieved by coating the pigment particles with transparent silica films (18). Aranzabe et al. (19) developed pigments based on a standard UB coated with different reflecting films, based on TiO_2, containing different types and concentrations of nanoparticles of alumina, titania and their mixtures. The pigments were dispersed in a water-based paint, stainless steel substrates were then painted with 50mm thick layer and the total solar reflectance (TSR) was measured. All of the obtained pigments increased the TSR of the original UB pigment.

There are references in the scientific literature that show the instability of the Ultramarine Blue pigments in cementitious media and evaluate the improvement of mechanical properties (20-22). They indicate the convenience of protecting the pigment by means of encapsulation or using additions with pozzolanic characteristics, to avoid the loss of colour. Giraldo et al. (23) delved into the pozzolanic properties of the pigment by replacing high percentages of white Portland cement (10 and 20%); attributing the reaction between the pigment and the portlandite to the formation of hauynite. They replaced the sodium ion for a calcium ion in the structure of UB, which would cause the disintegration and discoloration of the pigment samples.

The degradation process of the UB pigment in cementitious matrices involves a series of physical-chemical processes that the present work incrementally analyses in order to reveal the phenomenon that destabilizes the chromophore.

To evaluate the influence of different characteristic parameters of the cementing medium in the degradation process, the loss of colour of the pigment in solution was first addressed. Then, the influence of the pigment on the hydration of the cement and the formation of hydrated phases in cement pastes was studied. For this, two commercial UB pigments were used, one with, and the other without, a protective coating, in order to compare the degradation process in both.

2. MATERIALS AND METHODS

2.1. Materials

The samples initially used in the study were of pigment powder and then cement pastes incorporating the pigment. The cement used in the production of the different samples was a white cement BL I 52.5R. Its chemical composition is presented in Table1, with a specific gravity of 3060 g/cm^3 and a specific surface (Blaine) of 410 m^2/kg.

To carry out the studies, two commercially available ultramarine blue pigments (called UB0 and UB1) were used. The pigments studied were two different developments from the same company, being the pig-

ment UB1 a modification of UB0 by incorporating a protective encapsulation to prevent its degradation in cementitious media. This encapsulation was made by silicates and water-repellent additives. Table 1 shows the chemical composition (in the form of major oxides) of both pigments determined by XRF. It can be seen that the fundamental difference between pigment UB0 and UB1 is in the silicon, zinc and phosphorus contents, probably related to the encapsulation treatment to which pigment UB1 has been put through.

TABLE 1. Chemical composition of cement and pigments used.

Oxide content (%)	Cement	UB0	UB1
SiO_2	21.4	37.2	53.7
Al_2O_3	4.1	22.9	15.3
CaO	65.4	0.8	0.5
K_2O	0.6	0.9	0.4
Na_2O	0.1	19.4	13.0
SO_3	3.4	12.9	9.2
P_2O_5	-	0.1	1.4
ZnO	-		2.0
MgO	-	0.2	
BaO	1.3	0.4	0.6
TiO_2	-	0.02	0.1
Fe_2O_3	-	0.4	0.3
Rb_2O	0.3	0.02	
SrO	-	0.02	0.02
ZrO	-	0.02	
LoI	3.2	4.85	3.53

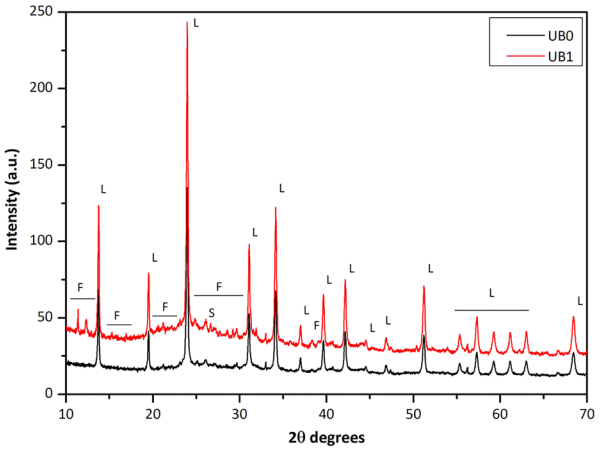

FIGURE 1. Diffractograms of the pigments studied.

The X-ray diffractograms of the pigments studied are shown in Figure 1. Most of the peaks detected correspond to a lazurite phase (L), which is characteristic of the ultramarine blue pigment. The Lazurite chemical formula is $Na_4Al_3Si_3O_{12}S$. The pigment sample UB1 presented another series of peaks, along with phase L, corresponding to zinc phosphate (F), and a halo between 20° and 30° 2θ that reveals the presence of amorphous components, probably amorphous silica due to the presence of spikes associated with silica (S) in the diffractogram.

2.2. Experimental program

To study the degradation of the pigments, an incremental study was carried out to analyse the pigments dissolution, as well as in pastes.

2.2.1. Study of pigment deterioration in different solutions

In the initial phase of the study, the process of colour loss of the pigment in solution was addressed, to evaluate the influence of different characteristic parameters of the cementitious medium in the degradation process (such as pH, alkali content and Ca^{2+} ion content).

Dissolution studies were carried out based on a modification of the method developed by Chinchón-Payá et al. (24) for the study of the oxidation of pyrites and pyrrhotites. Three different solutions were used, with a constant O_2 contribution, to study the above indicated parameters: a neutral solution (NS, medium only with water); a saturated solution of $Ca(OH)_2$, named SSC; and a solution that simulated the aqueous phase of the pores, named SSP (using KOH 0.6 mol/l; NaOH 0.2 mol/l; and $Ca(OH)_2$ until saturation). The solid / liquid ratio used was 1/20 (20 g of pigment per 400 ml of solution). The test duration was 60 days, during which the pH of the solution was periodically monitored. Likewise, samples of solution were extracted at 1, 3, 17 and 60 days for chemical analysis by ion chromatography and inductively coupled plasma – optical emission spectrometry (ICP-OES).

Through ion chromatography, the concentration of sulphates in the different media was monitored. The increase in sulphate concentration is directly related to the pigment degradation. As this occurs, the chromophore can get rid of the structure and oxidise. The following elements were analysed by ICP-OES: Na, K, Ca, Fe and Al. This allowed the analysis of the variation of its concentration as a function of the reaction time for the different media.

At the end of the test, the remaining solids were characterised by XRD, XRF and infrared spectroscopy and the results were compared with the analyses performed on the solid samples before beginning the dissolution analysis. Colorimetric analyses were also performed to determine the colour change in the samples.

2.2.2. Study of pigment deterioration in cement pastes

In the second stage of the experimental campaign, the evolution of the hydrated phases and the pigment in cement pastes were studied, using point and continuous DRX measurements. In order to do this, cement pastes were manufactured incorporating the pigments studied at 4% on the weight of the cement (w_c). In all the pastes, a fixed cement content (300 g) and a water/cementitious material ratio of 0.35 (corresponding to the amount of water necessary to obtain a normal consistency paste) were used.

2.3. Characterization techniques

2.3.1. X-Ray Diffraction measurement

Two types of XRD analysis were performed: point measurements and continuous measurements. For the point measurements, a PANalytical X'Pert PRO MPD Alpha1 was used, working in reflection with Bragg-Brentano geometry. CuKα radiation (λ = 1.5418 Å) filtered by Ni and an X'Celerator detector (active length of 2,122°), operating at 40 kV and 45 mA were used. The analysis conditions were between 4° 2θ to 80° 2θ, using an angular pitch of 0.017° 2θ and a step time of 50 seconds, with a variable divergence slit.

Continuous XRD measurements were performed following the same methodology used by Salvador et al. (25) to study the evolution of the hydration of cement pastes with setting accelerators. To this end, cement pastes were manufactured shortly before their measurement with an w/c ratio of 0.4, 4% w_c pigment. An internal alumina standard (NIST) was incorporated at 10% w_c. To avoid water evaporation during the measurements and carbonation of the samples, the sample holders were covered with a Kapton® film, with a thickness of 7.5µm. The temperature remained constant during the measurement process at 26 ºC. The measurements were made in a PANalytical X'Pert PRO MPD θ / θ device, working in reflection with Bragg-Brentano geometry. CuKα radiation (λ = 1.5418 Å), filtered by Ni, and a PIXcel detector (active length of 3,347°) were used, operating at 40 kV and 45 mA. Cylindrical sample holders, 32 mm in diameter and 3 mm deep, were used, which amounted to the use of approximately 3.7 g of paste for each test. The analysis conditions were between 5° 2θ and 70° 2θ, using an angular pitch of 0.026° 2θ and 60 seconds of passage time, with a fixed divergent slit of 0.5. A diffractogram was recorded every hour for the different samples, obtaining the first diffractogram 6 minutes after mixing the cement with the water. During the first 48 hours after mixing the cement with the water, diffractograms were obtained at the following times: 6 minutes, 1 hour, 12 hours, 24 hours and 48 hours. Once the continuous monitoring was completed, the samples were extracted and kept in containers with water, to facilitate the hydration process and to accelerate the possible degradation process. The samples, thus preserved, were maintained for a maximum of 24 days, obtaining diffractograms at 3, 5, 7, 10, 14, 17, 21 and 24 days. At the end of the study, all samples had lost the blue hue. The different diffractograms obtained were analysed qualitatively using X'Pert High Score Plus software.

2.3.2. Chemical analysis methods

The ICP analyses were performed with a Perkin Elmer Optima 4300DV Inductively Coupling Plasma emission spectrometer. The ion chromatography was carried out in a Dionex DX500 ion chromatography System. Likewise, quantification of the oxide content was carried out by X-ray fluorescence, in a sequential X-ray spectrometer (PHILIPS MAGIX PRO) equipped with a rhodium tube and beryllium window.

The characterisation of the solids before and after the experiment was carried out by infrared (IR) spectroscopy using an FT-IR Spectrometer (Bruker IF66 / S).

2.3.3. Colorimetric analysis

The analysis was conducted using an X-rite spectrophotometer (model RM200QC) with a measurement area of 8 mm in diameter, independent tri-directional 25 LED light source, D65 illuminant and an observer angle of 10º. Colour was expressed in the CIE L*a*b* space (26, 27). The parameters measured were the lightness L* (varying from black to white: 0 and 100, respectively), a* (which varies from +a* and –a*, red and green, respectively) and b* (with ranges from +b* and –b*, yellow and blue, respectively). The total colour change ΔE^*_{76} was computed using successive measurements performed at different times:

$$\Delta E^*_{76} = [(\Delta L^*)^2 + (\Delta a^*)^2 + (\Delta b^*)^2]^{1/2} \qquad [1]$$

where $\Delta L^* = L^*_t - L^*_1$; $Da^* = a^*_t - a^*_1$ and $Db^* = b^*_t - b^*_1$, which are the colour differences between age 1 and age t, according to the comparison of the colour before and after the exposure, respectively. For the purposes of the evaluation of the total color change, the criteria indicated in Table 2 were adopted, according to (26, 28, 29).

Table 2. Total colour change evaluation criteria.

ΔE^*_{76}	Visual assessment of ΔE^*
$0.5 < \Delta E^*_{76} < 1.5$	Slight
$1.5 < \Delta E^*_{76} < 3.0$	Obvious
$3.0 < \Delta E^*_{76} < 6.0$	Very obvious
$6.0 < \Delta E^*_{76} < 12.0$	Large

3. RESULTS AND DISCUSSION

3.1. Dissolution Testing

3.1.1. pH evolution

Figure 2 shows the evolution of pH with exposure time, depending on the type of sample and the environment studied. The medium with the highest pH value is the one that simulates the aqueous phase of the pores (SSP). In general, there is a decrease in pH in all media regarding values at early ages, although there are differences regarding the speed of change.

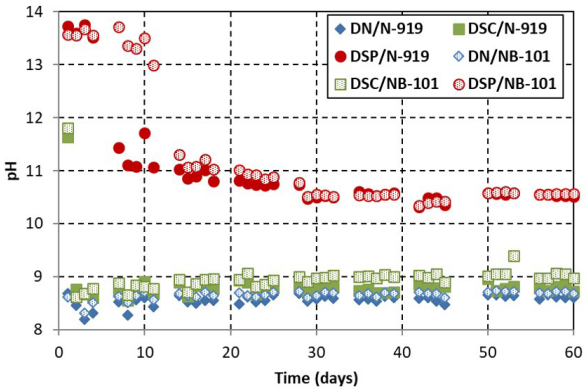

FIGURE 2. Evolution of pH in the different media studied.

The neutral solution (NS) and the saturated solution of calcium hydroxide (SSC) stabilised at a pH between 8.5 and 9.0, by the second or third days after starting the studies. In this sense, there are no significant differences in behaviour between the two pigments studied. The rapid and significant variation of pH in the SSC medium was equal to the pH values of the NS medium. The effect of CO_2 (carbonation) on pH decrease is clear in both SSC and SSP mixtures. The medium that simulates the aqueous phase of the pores (SSP) maintains high pH values for longer time due to larger amount of OH ions ($Ca(OH)_2$ has, by contrast, low solubility product). In this case stabilisation occurs around 20 days with a pH value close to 10.5. In this medium, behavioural differences are observed between the two pigments studied, the main one being the fact that it took twice as long for the UB1 sample to achieve pH stabilisation in relation to the UB0 sample (16 days and 8 days, respectively).

3.1.2. Ion chromatography

The sulphate concentration in the different media is monitored by ion chromatography. Figure 3 shows this variation depending on the type of sample, medium and time of sampling. Each value represented in Figure 3 is the mean of the results of 5 samples, the coefficients of variation obtained by a basic statistical analysis of the results in all cases were less than 1%.

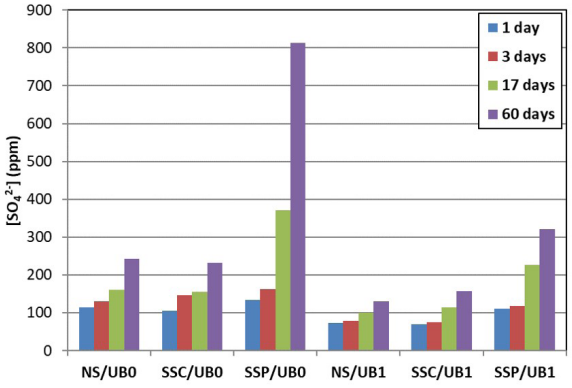

FIGURE 3. Evolution of the sulphate concentration in the different media studied.

In all of the samples studied, an increase in the sulphate content occurs with the exposure time. However, this increase is more noticeable in the UB1 pigment samples and in the samples exposed to the solution that simulates the aqueous phase of the pores (SSP). These results show the different behaviour of both pigments, as well as the different aggressiveness of the solutions under study.

3.1.3. ICP-OES

The following elements have been analysed using the ICP-OES technique: Na, K, Ca, Fe and Al. Table 3 shows the variation of its concentration as a function of the reaction time. It is worth noting that Fe ion was not detected in any of the solutions.

First, the variation of the calcium ion content will be analysed. The variations obtained differ significantly depending on the medium, so they will be analysed separately. On the one hand, the samples contained in the neutral solutions (NS) hardly show any increase in the calcium content, with only minor increases occurring for the UB0 sample. On the other hand, saturated solutions of calcium hydroxide (SSC) show significant differences in calcium ion content between both pigments. Considering that it initially started from a concentration of 1850 ppm of calcium in solution (saturated medium), the decrease in calcium content in solution may be due to both environmental carbonation and the incorporation of the calcium ions into the pigment structure. The differences obtained between the pigment samples show a reaction of the calcium in solution with the pigment, which was much more significant in the UB0 sample. Finally, in the SSP medium, the observed behaviour is anomalous a priori. For both samples studied, during the first few days, it was not possible to detect calcium in solution; subsequent measurements showed an increase in its

Table 3. Concentration of the cations in each of the solutions.

Media	Time (days)	Ca (ppm)		K (ppm)		Na (ppm)		Al (ppm)	
		UB0	UB1	UB0	UB1	UB0	UB1	UB0	UB1
SN	1	0.722	0.0	2.2	1.4	107	120	0.577	0.034
	3	0.828	0.376	7.0	8.1	149	150	0.717	0.037
	17	1.664	0.15	11.1	2.4	204	187	1.1	0.149
	60	0.854	0.0	5.5	2.3	268	237	0.590	0.207
SSC	1	3.9	62.2	12.5	10.8	120	64	9.5	0.163
	3	14.8	51.9	3.4	1.6	150	123	0.884	0.011
	17	7.1	61.0	5.1	2.7	187	224	1.6	0.036
	60	6.1	35.3	5.9	2.9	237	329	1.3	0.145
SSP	1	0.0	0.0	19420	20070	5250	5358	174	9.9
	3	0.0	0.0	21260	19790	6087	5480	203	11.8
	17	71.9	20.3	25500	24120	8666	7344	11.0	2.6
	60	0.0	6.5	33200	33900	13100	11200	11.3	0.0

concentration and a subsequent disappearance or decrease.

In the case of the variation of the potassium ion content, the variations are significantly different depending on the type of medium. In the neutral solution and that saturated with calcium hydroxide there are very low contents of this ion (below 13 ppm in all cases). The variations observed in these cases are within the detection limit of the technique and cannot be attributed to specific behaviours. The solution that simulates the aqueous phase of the pores (SSP) shows an increase in the potassium ion content in solution throughout time, without appreciating significant differences between both pigments.

Studies carried out by Booth et al. (8) revealed that the modification in cation type and content in the pigment structure leads to an increase in the size of the unit cell (larger structures), and also to interactions between the cations and the chromophore that can lead to a colour change. Based on the data in Table 1, the potassium content in the pigments was less than 1%. Likewise, the initial content of potassium ion in solution was 24,000 ppm (0.6 mol / L). The K concentration increase in SSP along time, evidencing a possible ion-exchange phenomenon between the pigment and the solution.

The variation in sodium ion content shows similar trends for the different samples and media studied, as can be seen in Table 3. In all cases, a continuous increase in the sodium ion content is observed throughout time, both in the UB0 sample and in UB1.It is noteworthy that the ion content that is present in solution differs significantly between the samples exposed to the medium that simulated the aqueous phase of the pores (SSP) and the rest of the samples (NS and SSC). The initial sodium ion content in that medium was approximately 4,600 ppm, which shows the ion exchange process that is taking place.

Finally, by analysing the aluminium ion content in a general way, in the different samples and media studied, it can be seen that its variation is minor, with the exception of the samples exposed to the medium that simulates the aqueous phase of the pores (SSP). In this medium, both UB0 and UB1 show an increase in the content of aluminium ions in the first 3 days subsequently, show a reduction. In the case of UB0 it goes from a concentration of 203 ppm to one of 11 ppm. This abrupt variation in the content of the aluminium ions may be related to some precipitation or reaction process.

The results presented show that:

- An ion exchange phenomenon occurs. This ion exchange takes place between the sodium ions of the pigment and the calcium and potassium ions present in the different media, without ruling out the existence of other ions or impurities present in the pigments that could also contribute to this phenomenon.
- The ion exchange takes place in the three studied media, with different extensions in each one of them. When potassium ions are present (as is the case with the medium that simulated the aqueous phase of the pores, SSP), it takes place to a greater extent.
- Only the samples exposed to the SSP environment have shown evidence of modification of the aluminosilicate structure that makes up the pigment cell. This modification has been confirmed by the presence of aluminium contributed to the solution after the degradation of the pigments and the higher concentration in the samples exposed to the SSP medium at 1 and 3 days.

3.1.4. Solids analysis

Different samples of solids were taken at the same times as the aliquots for the solutions analyses (at 1, 3, 18 and 60 days). The results obtained by XRD and XRF were compared to analyses carried out on the

solid samples before beginning the dissolution analyses. Similarly, infrared spectroscopy analyses were performed on both non-degraded pigments and the final solids of each of the degradation experiences (after 60 days of exposure). The results obtained are presented and discussed below.

Diffractograms obtained for both pigments preserved in the neutral solution (NS), at the different ages studied, did not show significant differences, being consistent with the results of the analysis of the solutions, where no significant changes were evident.

Diffractograms of the samples of both pigments exposed to the lime saturated solution (SSC) showed some differences compared to the untreated sample. The main difference found was the appearance of new peaks at different angular spacings, in the 29 to 30 ° 2θ and 43 to 50 ° 2θ intervals in the UB0 pigment, and in the first interval only in the UB1 pigment. These corresponded to the presence of calcite and could be induced during sample preparation of UB0 for the XRD; in pigment UB1 they were less noticeable than in UB0.

Diffractograms of the two pigments that were exposed to the SSP medium, showed greater differences. The main variations were in relation to the intensity losses in the peaks (displacement to 2θ lower values and an increase in the width of the peaks) as the exposure time of the pigments in solution progresses. The effect of the degradation process is shown in Figure 4, with the variation of the intensity and spacing of the peak located at 24 ° 2θ.

The decrease in the intensity of the peak shows that the crystalline structure is changing, while the modification of spacing *d* indicates that an increase in the size of the unit cell (and its distortion) is taking place.

As the degradation process progresses, the structure degrades, as shown in Figure 4b. This modification leads to destabilisation and oxidation of the S_3^- chromophore and, therefore, to loss of pigment colour.

The analysis of both parts of the figure shows that the degradation phenomenon occurs more significantly in UB0 than in UB1, although both samples show evidence of modifications in their crystal structure. The modification that takes place is a distortion of the lazurite-like structure of the pigment and a loss of crystallinity, this may be associated with the formation of a new phase.

Figure 5 shows the diffractograms of UB0 and UB1 after times 0 and 60 days in the SSP medium, showing the coincidences with the hauynite phase (showed as dashed lines on the diffractograms). Previous results presented by Giraldo (23) also evidenced the formation of this phase. The new phase that is formed could be related to hauynite, since the displacement of the

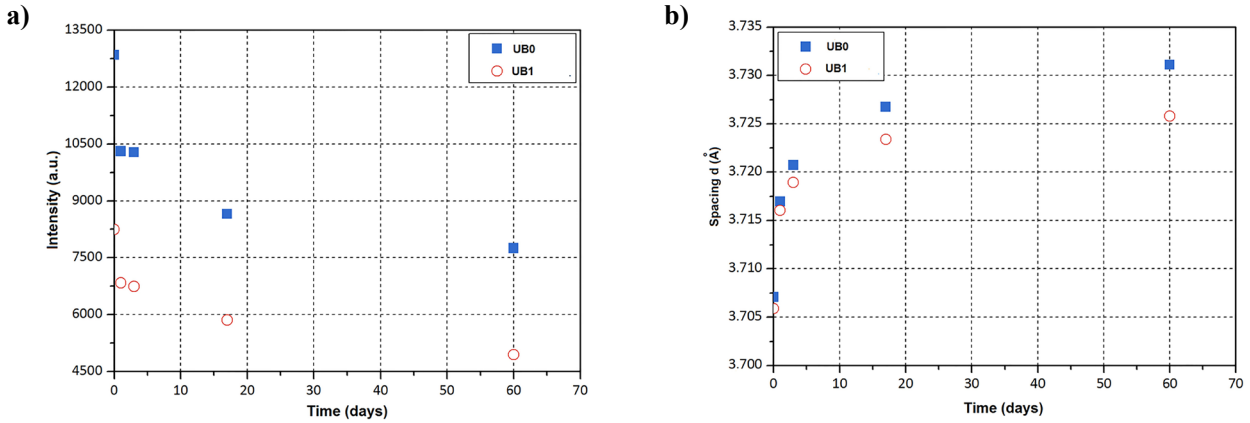

FIGURE 4. Modification of the main peak (24 ° 2θ): a) intensity; b) spacing d.

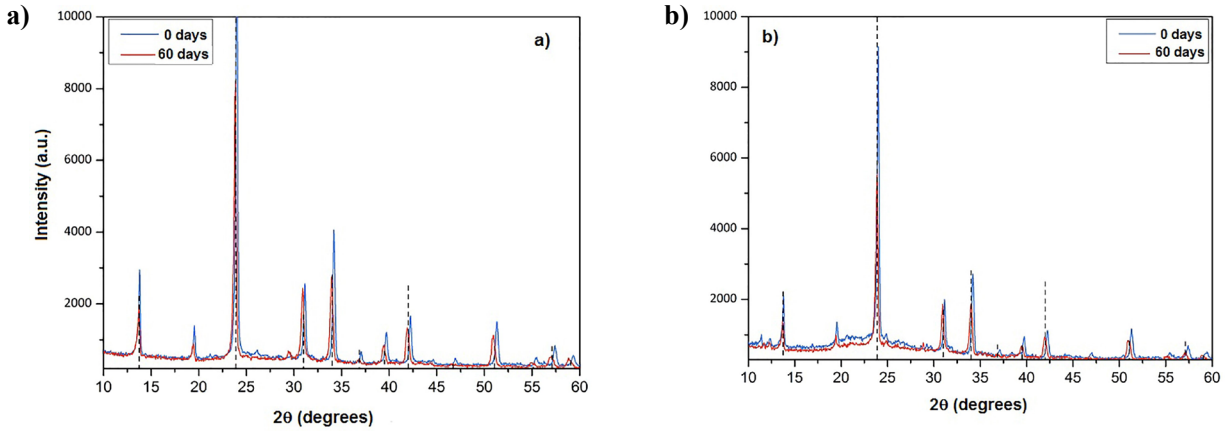

FIGURE 5. Hauynite phase formation in samples degraded in the SSP medium: a) UB0; b) UB1.

peaks coincides with that of this phase and has the chemical formula: $K_{1,6}Ca_{2,4}Na_{4,32}(Al_6Si_6O_{24})(SO_4)_{1,52}$. It is also an alumino-silicate, but has incorporated calcium and potassium into its structure.

The degradation of the pigment structure is observed in the X-ray diffractograms. Peak modifications have been noted, as well as distortion of the unit cell. According to (3), the diffractograms of the samples depend fundamentally on the structure of the aluminosilicate. Ultimately, it is this modification of the aluminosilicate structure that favours the loss of colour of the pigment.

The chemical composition of the solids obtained after 60 days of treatment was determined by means of X-ray fluorescence and compared with the untreated samples of the pigments. Likewise, the loss on ignition (LOI) of the different samples was determined. The results obtained are shown in Table 4, for the different environments studied.

It is worth noting that the pigments were mainly composed of silicon, sodium and sulphur, as shown in Table 1, and that they hardly showed any trace of calcium or potassium in their composition.

Firstly, the variation of aluminium and silicon content was analysed, since it may show modifications in the structure of the zeolite that contains the chromophore. In both cases, the observed variations do not clearly show the effect of the degradation process.

It must be taken into account that X-ray fluorescence provides contents in percentages, so the variation of one of the components can affect the others. In this sense, the analysis of the Si/Al ratio in the pigment can provide more information on the degradation phenomenon, as can be seen in Table 4. This relationship hardly varies in the UB0 samples while there is a slight variation in the UB1 samples exposed to SSC and SSP environments, showing a slight loss of aluminium in the structure.

The analysis of the other major pigment component, sodium, shows that, in both pigments, the samples exposed to the SSP environment show significant reductions in its content. In the analysis of the major components of the pigments, it is worth noting the variation in the sulphur content. In this sense, a noticeable decrease in the sulphur content is observed for all samples and studied environments, although in SSP this decrease was the smallest. In ultramarine pigments, sulphur can be found in the form of a chromophore (S_3-) or in the form of a sulphate ion (7), the former providing the blue colour to the pigment. The sizes of the two ions differ markedly, and probably this difference in size allows ion exchange of the sulphate anions to take place in all of the media studied.

Another factor to consider is the loss on ignition (LoI), which makes evident the presence of hydrated or carbonated compounds in the pigments. The results obtained show increases in these in all environments, being more remarkable in the samples exposed to the SSP environment. This fact could be the result of the reaction or incorporation of calcium, in the form of portlandite, to the pigment and its subsequent carbonation with ambient CO_2. The modification of the aluminosilicate structure that makes up the pigment cell, has been confirmed by the decrease in the contents of the major components studied in the pigments.

After this, the content variation of the minority elements (calcium, potassium and phosphorus) was analysed. Regarding calcium, there is a remarkable increase in content in samples exposed to the medium saturated with lime (SSC). This fact may be related to the incorporation of this ion into the pigment structure. It is noteworthy that this increase is not seen in the samples exposed to the medium that simulated the aqueous phase of the pores (SSP).

Potassium also shows a remarkable increase in content, in the samples exposed to the medium that simulated the aqueous phase of the pores (SSP); the samples exposed to the other environments do not show significant variations in the content of this element compared to the untreated sample UB0. As previously showed by Booth et al. (8), the ion-exchange phenomenon between the SSP solution and the pigment may lead not only to an increase in the size of the unit cell (larger structure), but interactions between the cations and the S^{3-} chromophore may also

Table 4. Chemical composition (%) of the samples obtained after the studies in solution.

	CaO	Al_2O_3	SiO_2	SO_3	P_2O_5	Na_2O	K_2O	LoI	Si/Al
UB0	0.8	24.1	39.1	13.6	0.1	20.4	0.9	4.9	1.63
NS/UB0	0.8	27.1	43.9	4.8	0.1	20.9	1.2	10.2	1.62
SSC/UB0	3	26	42	5	0.1	20	1	11.8	1.59
SSP/UB0	1	24	40	7	0.1	16	10	35.2	1.64
UB1	0.5	15.9	55.7	9.5	1.5	13.5	0.4	3.5	3.51
NS/UB1	0.5	17.5	57.9	4.5	1.6	13.9	0.7	12.0	3.30
SSC/UB1	2.0	15.6	59.2	4.9	1.6	12.9	0.5	8.3	3.80
SSP/UB1	0.8	14.2	53.9	7.8	0.9	10.7	9.1	13.2	3.80

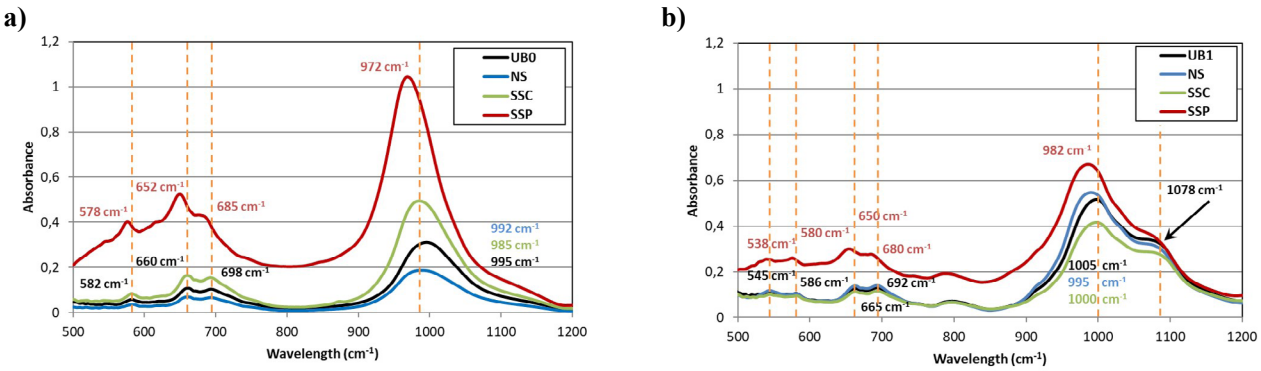

FIGURE 6. IR spectra before and after 60 days of exposure to the different environments of the samples: a) UB0; b) UB1.

take place, which at the end can lead to the colour change that is experimentally observed.

The presence of phosphorus in the UB1 pigment samples is interesting. The diffractograms of the untreated samples, shown in Figure 1, evidenced the presence of some type of inorganic phosphate in these samples. Table 4 shows a decrease in the phosphorus content in the UB1 pigment samples exposed to the environment that simulated the aqueous phase of the pores (SSP), compared to the original samples; the possible degradation of the coating pigment protector is evident.

Figures 6a and 6b show the different IR spectra obtained for samples UB0 and UB1 before and after exposure to the different environments evaluated. To facilitate interpretation, only the information contained between wavelengths 500 to 1200 cm^{-1} is presented.

Figure 6a clearly shows that the spectra obtained from the UB0 pigment are characteristic of aluminosilicates. The characteristic peaks of the S_3- chromophore are located at 542 and 582 cm^{-1} (30, 31); in this pigment only the peak at 582 cm^{-1} is observed. Similar results have been obtained (32), showing an intense band in that location. In this area, a certain modification in the IR spectrum can be seen in the Figure. Samples exposed to neutral and lime saturated solutions do not undergo significant modifications. However, the sample exposed to the solution that simulated the aqueous phase of the pores shows a shift of the chromophore peak to 578 cm^{-1}.

The peaks that appear in the 650-700 cm^{-1} band and the intense peak that appears around 1000 cm^{-1} are characteristic of the Si-O-Al bonds of the aluminosilicates (33). In NS and SSC media, there are few modifications in these bands but slight variations in intensity in the 1000 cm^{-1} band, which increases in intensity in the SSC medium and moves to values close to 990 cm^{-1}. This may show the incorporation of Ca^{2+} ions in the aluminosilicate structure. The most significant changes are seen in the sample exposed to the SSP environment. In addition to an outstanding increase in the intensity of the band at 1000 cm^{-1} and a shift to values close to 970 cm^{-1}, an outstanding distortion of the band 650-700 cm^{-1} is observed in Figure 6a. These differences reveal alterations in the Si-O-Al bonds, due to the pigment degradation process.

When analysing the spectra obtained for the UB1 sample (see Figure 6b), no significant differences were observed between the different media. There are hardly any differences between the samples exposed to the NS and SSC media, regarding the starting sample. The sample submitted to the SSP medium presents a series of differences that are similar to those found in the UB0 sample, although less intense. The different changes observed are related to the distortion of the structure of the chromophore and of the Si-O-Al bonds of the aluminosilicates.

The shoulder seen around 1100 cm^{-1} (marked with an arrow in Figure 6b is related to Si-O-Al bonds, probably due to the amorphous or polymeric silica used in the coating of the UB1 sample. These results agree with previously published results (17).

3.1.5. Colorimetric analysis

The results of the colorimetric analysis of the samples of pigments UB0 and UB1 as well as those of the final solids of all the degradations studied in solution, are presented in Table 5 where the values obtained by the CIE L* a* b colour system are collected, and then represented in Figure 7. In Table 5, it can be clearly seen that the major colour differences ΔE^*_{76} occur in pigment UB0 exposed to the medium that simulates the aqueous phase of the pores (SSP), where $\Delta E^*_{76} >> 12$.

3.2. Studies on pastes

3.2.1 Evolution in early and long-term stages

First of all, the evolution of the samples in early stages was analysed during the first 48 hours after mixing the material. The following study intervals were selected: 0.10 hours (first measurement performed), and then 1, 12, 24 and 48 hours. Figure 8 shows the evolution of the hydration of the cement pastes with the two pigments studied at the indicated ages. The

TABLE 5. Colorimetric analysis of each of the samples analysed.

Pigment	Legend	Solution	L*	a*	b*	ΔE^*_{76}	Visual assessment Of ΔE^*_{76}
UB0	■	Initial	51.16	15.75	-39.02		
	●	NS	50.27	14.64	-35.45	3.84	Very obvious
	▲	SSC	50.80	15.34	-37.34	1.77	Obvious
	▲	SSP	47.45	12.17	-26.89	13.18	Very large
UB1	△	Initial	53.24	15.16	-40.23		
	□	NS	51.15	14.17	-35.32	5.43	Very obvious
	○	SSC	51.62	13.77	-35.54	5.15	Very obvious
	●	SSP	49.60	14.49	-33.17	7.90	Large

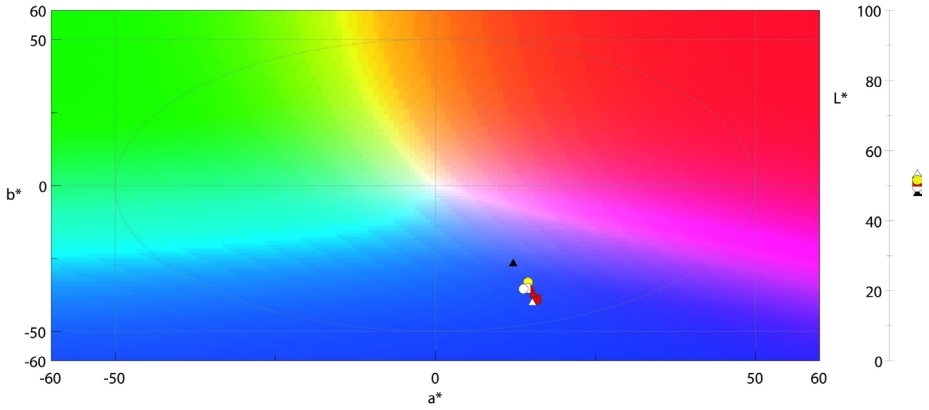

FIGURE 7. Visualization of colorimetric results using the CIE L * a * b colour system.

main modifications in the diffractograms appear in the range 5 ° to 30 ° 2θ, in which the main detected phases have been indicated in the cited figure: Et – Ettringite, M – Monocarboaluminate, G-Gypsum, P – Portlandite, C – Calcite, L – Lazurite, A – Alumina and Q – Quartz. From this angle, the variations correspond mainly to the unreacted cement.

As the hydration process progresses, as is clearly seen in Figure 8a, portlandite, ettringite and monocarboaluminate appear as the main products of cement

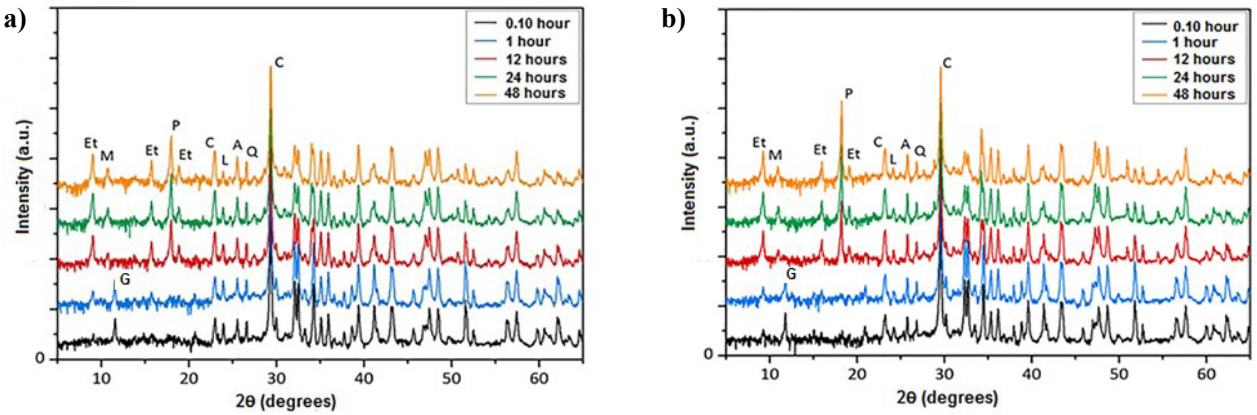

FIGURE 8. Evolution of pastes with pigments at early stages: a) UB0; b) UB1.

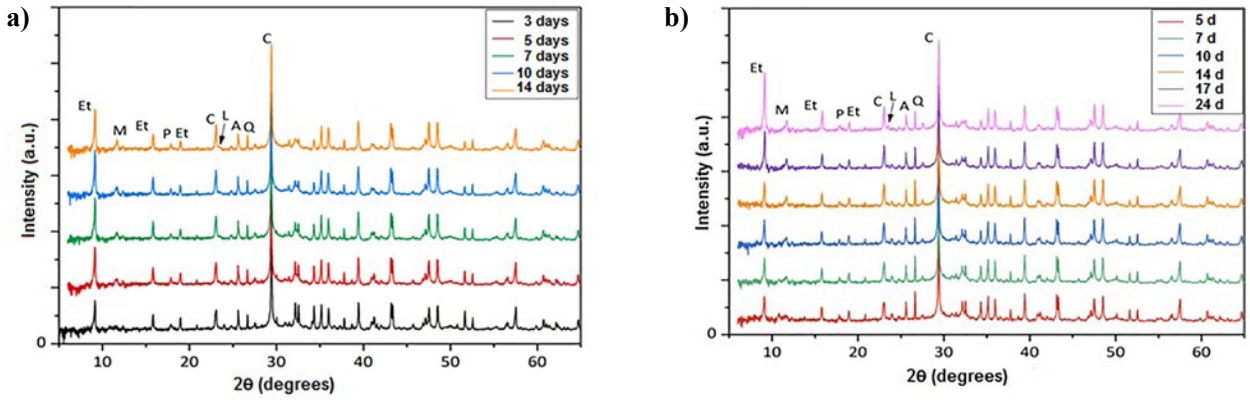

FIGURE 9. Long-term evolution of pastes with pigments: a) UB0; b) UB1.

hydration. Likewise, and as one would expect, the disappearance of the gypsum is observed between 1 and 12 hours after manufacturing. The other phases present are calcite, alumina (used as an internal standard) and quartz. Figure 8b shows the evolution of the hydration of the cement paste with the UB1 pigment in the initial stages. The phases identified are the same as those found in the paste with UB0 pigment. For at least up to 48 hours, higher ettringite contents are not appreciated, as stated in the bibliography (22, 23).

3.2.2. Long-term evolution

Once the continuous monitoring was completed, the pastes were kept in containers with water, as indicated in Section 2.3.2. In relation to the long-term evolution Figure 9 shows diffractograms of the samples made with pigments UB0 and UB1, indicating the main phases detected.

In the samples made with the UB0 pigment (as shown in Figure 9a), the abundant presence of ettringite stands out. The low intensity of the portlandite peak is also noteworthy, especially in the younger samples (3 days) that have been less exposed to environmental carbonation. Finally, it is worth highlighting that the evolution of the pigment degradation process between 10 and 14 days, is not possible to practically detect the peak with the highest intensity. The diffractograms of the samples made with the UB1 pigment present a similar scenario, as shown in Figure 9b. High ettringite contents and low portlandite contents can be repeatedly seen in all of the analysed stages. It is noteworthy that the intensities of the ettringite peaks are higher in the samples with UB1 pigment than in the samples with UB0 pigment. The peak corresponding to the pigment is appreciable for a longer time, although at 24 days its intensity is practically negligible, revealing that degradation has taken place. As a reference element, the diffractograms of the long-term pigment-free cement pastes are shown in Figure 10. Of the mentioned figure, two aspects should be highlighted: the absence of peaks corresponding to ettringite and the portlandite content.

Regarding ettringite, and in light of previous comments on the cement hydration process, it disappears 3 days after the sample is manufactured, as can be seen in Figure 10. Instead, we found the presence of various phases of monosulfoaluminate and monocarboaluminate. As sample curing progresses, the intensity of the peaks in these phases increases. Therefore, the diffractograms obtained at 21 days for the reference sample contrast with those obtained for pastes with different pigment samples. In all the pigmented samples we found high ettringite contents and the intensity of the peak of the monosulfoaluminate / monocarboaluminate phases is lower than in the reference samples.

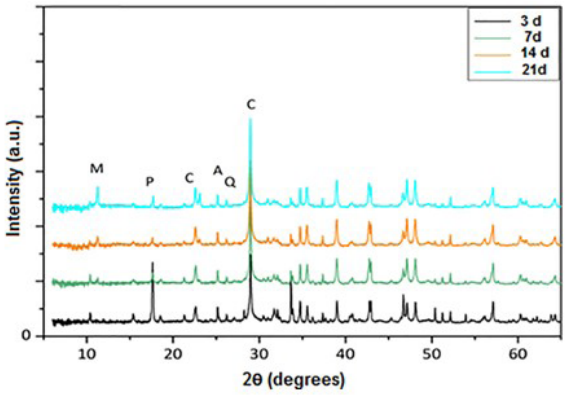

FIGURE 10. Long-term evolution of reference pastes (without pigment).

The intensity of the portlandite peak at 3 days stands out compared to that observed in the pastes with the different pigment samples. The intensity observed in Figure 10, as well as its evolution over time, responds to the normal process of cement hydration and carbonation of the sample as it is preserved in laboratory conditions and exposure to environmental CO_2.

3.2.2 Semi-quantitative analysis

Complementary to the results shown in the previous section, and to facilitate the interpretation of

the results, a semi-quantitative analysis of the evolution of the content of each phase was performed. For this, the internal standard added in each sample was used, in a known quantity. As this is an inert phase, its intensity must be constant and vary according to the experimental conditions of the diffractograms.

In this way, it is possible to obtain relative intensities. Table 6 shows the main data from the different phases analysed. The calculation of the relative intensities of the different phases has been performed according to Equation [2], in which I_i is the intensity of the main peak of the phase concerned (in calculation) and is the intensity of the main peak of the internal alumina standard (in calculation).

$$\text{Rel. Int.} = \frac{I_i}{I_{Al_2O_3}} \qquad [2]$$

TABLE 6. Relation of the analysed phases and applied parameters.

Phase	Formula	Code PDF	Main peak (° 2θ)
Alumina	Al_2O_3	010-0173	43.36
Calcite	$CaCO_3$	083-0577	29.41
Portlandite	$Ca(OH)_2$	072-0156	18.11*
Ettringite	$Ca_6Al_2(SO_4)_3(OH)_{12}\cdot 26H_2O$	041-1451	9.09
Ultramarine blue	$A_n((Al, Si)_{12}O_{24})X_2$	041-1393	38.76

* Portlandite, along with other hydrated phases, usually has a preferred orientation of certain reflection planes. This causes that the most intense peak is not the one outlined in the crystallographic record, but the one indicated in Table 6.

Figure 11 shows the variation of the relative intensities of the phases of interest (portlandite, ettringite, calcite and pigment) for pastes containing the two studied pigments.

The results corresponding to the pastes with pigment UB0 (Figure 11a), show that, firstly, the ettringite content increases continuously during the study time, stabilising between 7 and 10 days. On the contrary, the content of portlandite increases during the initial period, up to its maximum at 48 hours, then it decreases drastically until it is practically undetectable on the diffractogram.

Figure 11a shows that the content of the UB0 pigment decreases continuously from the beginning, reaching the minimum between 2 and 3 days. Subsequently it remains at a level close to the detection limit.

These results contrast with those that can be seen for the samples with the pigment UB1, whose variation of relative intensities over time is presented in Figure 11b. The most remarkable differences are found in the ettringite and portlandite contents.

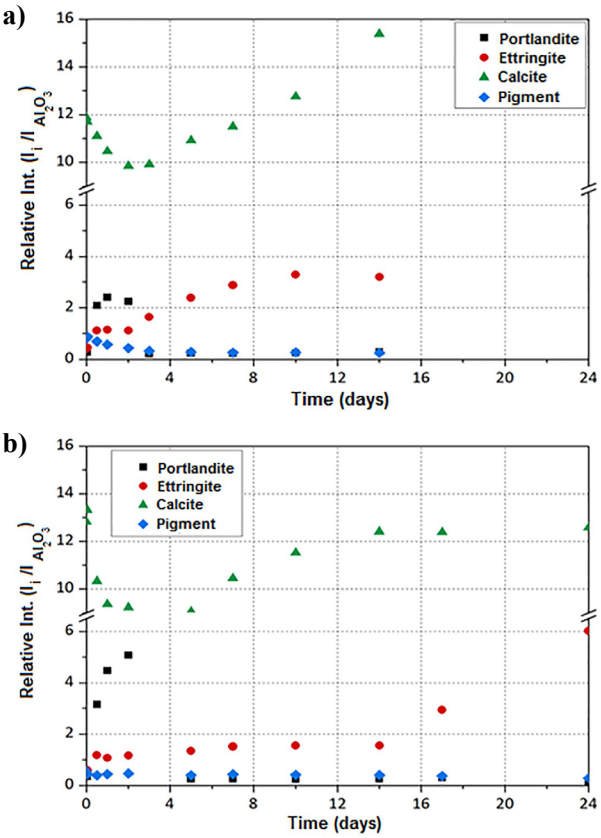

FIGURE 11. Variation of relative intensities over time of crystalline phases in pigmented samples: a) UB0; b) UB1.

Regarding the first, the contents in early ages are similar to those observed in the sample with pigment UB0. However, although there is an increase in the ettringite content over time, it is not as remarkable as the one observed in the sample with pigment UB0. An increase in the ettringite content is only observed in the sample after 14 days, reaching values much higher than those observed in the sample with UB0 pigment. This phenomenon reveals the formation of ettringite from monosulfoaluminate phases and at an age in which the rigidity of the material is high. It should be borne in mind that the formation of ettringite from these phases is an expansive process, due to the difference in volume between the two phases. This could become a durability problem for materials containing this pigment.

Regarding portlandite, its contents are observed in the early ages and are much higher than those found in the sample with UB0 pigment, which shows the different reactivity of both pigments. Finally, regarding the pigment content, Figure 11b shows only a slight variation of the same. It should be noted that the starting intensity of the pigment peak was already lower, which influences the subsequent detection process. At the end of the measurement process, it was practically impossible to detect the pigment peak.

4. CONCLUSIONS

4.1. General conclusion

The incremental study presented allows us to conclude that the process of degradation of the ultramarine blue pigment in cementitious media mainly attends to a process of reaction and ion exchange. During hydration, high ion contents are released, with calcium and potassium being the most aggressive for UB pigments.

Calcium is incorporated into the aluminosilicate structure, distorting the unit cell. A cation exchange phenomenon occurs between the sodium in the pigment and the potassium in the medium. Both processes lead to the diffusion of sulphate and sulphide ions from the pigment to the cementitious medium, and thus the chromophore S^{3-} is degraded leading to a colour loss. In the end, it is this phenomenon of diffusion of sulphate ions that causes the formation o ettringite in the studied material. This formation of ettringite could have other consequences, depending on the moment of formation in the material, since it is, in some cases, an expansive phenomenon.

4.2. Conclusions of the dissolution studies

The dissolution studies presented in Section 3.1 allowed us determine the aggressiveness of different conditions and identify the degradation processes that were taking place.

The different results obtained allow us to conclude that the most aggressive samples of the ultramarine blue pigment are obtained with the medium that simulated the aqueous phase in the pores (SSP). This aggressiveness leads to the degradation of the pigments to a greater extent. Likewise, it has been concluded that the pigment with a protective coating (UB1) resists the aggressive environment better than the one without it (UB0), although it also suffers degradation.

4.3. Conclusions of the studies on cement pastes

The studies of cement pastes were aimed at monitoring the hydration process of the pastes with the incorporation of the ultramarine blue pigment. This allowed us to carry out an in-depth analysis of the degradation process that takes place, see Section 3.2.

Degradation takes place in three different phases. In phase one, calcium is incorporated into the pigment's aluminosilicate structure, distorting it. In phase two, a cation exchange takes place between the pigment's sodium and the potassium present in the cementitious medium. In phase three, and as a consequence of the previous two, sulphate and sulphide ions are diffused into the medium, leading to the stabilisation of the primary ettringite and the formation of secondary ettringite. Occasionally, this phenomenon could give rise to some expansive phenomenon, being a type of internal sulphate attack.

Acknowledgments

The authors would like to thank the company Nubiola for the help provided in the development of this research.

Funding Sources

Research carried out within the framework of Project BIA2013-49106-C2-1-R, "Gestión y seguridad en infraestructuras. hidraulicas", financed by the Spanish Ministry of Economy and Competitiveness through Project. Furthermore.

Authorship contribution statement

Gemma Rodríguez de Sensale: Writing – original draft.

Viviana de Lima: Investigation.

Servando Chinchón-Paya: Investigation.

Antonio Aguado: Conceptualization, Funding acquisition, Writing – review & editing.

Ignacio Segura: Conceptualization, Methodology, Project administration, Supervision, Investigation, Writing – review & editing.

The authors of this article declare that they have no financial, professional or personal conflicts of interest that could have inappropriately influenced this work.

REFERENCES

1. Osticioli Y, Mendes NFC, Nevin A, Gil PSC, Becucci M, Castelluci E. 2009. Analysis of natural and artificial ultramarine blue pigments using laser induced breakdown and pulsed Raman spectroscopy, statistical analysis and light microscopy. Spectrochim. Acta Part A. Mol. Biomolec. Spectros. 73(3):525-531. https://doi.org/10.1016/j.saa.2008.11.028.
2. Plesters J. 1966. Identification of materials of paintings: II. Ultramarine blue, natural and artificial. Studies in conservation. 11(2):76-91.
3. Landman AA. 2003. The role sulphur plays in the formation of ultramarine blue, in: University of Pretoria ed., Aspects of solid-state chemistry of fly ash and ultramarine pigments, PhD These, Chapter 4, Pretoria, 65-76.
4. Arieli D, Vaughan DEW, Golfarb D. 2004. New synthesis and insight into the structure of blue ultramarine pigments. J. Amer. Chem. Soc. 126(18):5776-5788. https://doi.org/10.1021/ja0320121.
5. Miliani C, Daveri A, Brunetto BG, Sgamellotti A. 2008. CO_2 entrapment in natural ultra-marine blue. Chem. Phys. Lett. 466(4-6):148-151. https://doi.org/10.1016/j.cplett.2008.10.038.
6. Cato E, Rossi A, Scherrer N, Ferreira ESB. 2018. An XPS study into sulphur speciation in blue and green ultramarine. J. Cult. Herit. 29:30-35. https://doi.org/10.1016/j.culher.2017.09.005.
7. Climent-Pascual E, Sáez-Puche R, Gómez-Herrero A, Romero J. 2008. Cluster ordering in synthetic ultramarine pigments. Micropor. Mesopor. Mater. 116(1–3):344–351. https://doi.org/10.1016/j.micromeso.2008.04.026.

8. Booth DG, Dann SE, Weller MT. 2003. The effect of the cation composition on the synthesis and properties of ultramarine blue. Dyes Pigmen. 58(1):73-82. https://doi.org/10.1016/S0143-7208(03)00037-8.
9. Cato E, Borca C, Huthwelker T, Ferreira ESB. 2016. Aluminium X-ray absorption near-edge spectroscopy analysis of discoloured ultramarine blue in 20th century oil paintings. Microchem. J. 126:18-24. https://doi.org/10.1016/j.microc.2015.11.021.
10. Plesters J. 1993. Ultramarine blue, natural and artificial, in: ashok roy ed., artists pigments: a handbook of their history and characteristics, vol. 2, National Gallery of Art, Washington, 37-65.
11. Del Federico E, Newman J, Tyne L, O'Hern C, Isolani L, Jerschow A. 2006. Solid-state NMR studies of ultramarine pigments discoloration. MRS Online Proceedings Library Archive 984, 713. https://doi.org/10.1557/PROC-984-0984-MM07-13.
12. Del Federico E, Shöfberger W, Schelvis J, Kapetanaki S, Tyne L, Jerschow A. 2006. Insight into framework destruction in ultramarine pigments. Inorg. Chem. 45(3):1270-1276. https://doi.org/10.1021/ic050903z.
13. De la Rie ER, Michelin A, Ngako M, Del Federico E, Del Grosso C. 2017. Photo-catalytic degradation of binding media of ultramarine blue containing paint layers: A new perspective on the phenomenon of "ultramarine disease" in paintings. Polym. Degrad. Stab. 144:43-52. https://doi.org/10.1016/j.polymdegradstab.2017.08.002.
14. Cato E, Scherrer N, Ferreira ESB. 2017. Raman mapping of the S3-chromophore in degraded ultramarine blue paints. J. Raman Spectros. 48(12):1789-1798.
15. Gobeltz N, Demortier A, Lelieur JP, Duhayon C. 1998. Encapsulation of the chromophores into the sodalite structure during the synthesis of the blue ultramarine pigment. J. Chemic. Soc. Farad. Transac. 94(15):2257-2260. https://doi.org/10.1039/A801526K.
16. Liu QX, Xu ZH, Finch JA, Egerton RA. 1998. A novel two-step silica coating process for engineering magnetic nanocomposites. Chem. Mater. 10(12):3936-3940. https://doi.org/10.1021/cm980370a.
17. Li S, Liu M, Sun I. 2011. Preparation of acid-resisting ultramarine blue by novel two-step silica coating process. Industr. Engineer. Chem. Res. 50(12):7326-7331. https://doi.org/10.1021/ie200343k.
18. Liu M, Li S, Umereweneza D. 2011. Enhancement of acid resistance for ultramarine blue by silica coatings. Advanc. Mater. Res. 291-294:163-166. https://doi.org/10.4028/www.scientific.net/AMR.291-294.163.
19. Aranzabe E, Villasante PM, March R, Arriortua MI, Vadillo J, Larrañaga A, Aranzabe A. 2016. Preparation and characterization of NIR reflective pigments based in ultramarine blue. Ener. Build. 126:170-176. https://doi.org/10.1016/j.enbuild.2016.05.011.
20. Kroone B. 1968. The reaction between hydrating Portland cement and ultramarine blue. Chemistry and Industry. London, 287-288.
21. Posada N, Sanmartín R, Restrepo O. 2003. Coloración de cemento con pigmento azul ultramar. DYNA 70(139):35-45. Retrieved from https://www.redalyc.org/articulo.oa?id=49613905.
22. Restrepo J, Restrepo O, Tobón O. 2009. Evaluación del desempeño mecánico del cemento blanco coloreado con pigmento azul ultramar. DYNA 76(157):225-231. Retrieved from https://revistas.unal.edu.co/index.php/dyna/article/view/9571/11501
23. Giraldo C, Tobón JI, Restrepo OJ. 2012. Ultramarine blue-pigment: A non-conventional pozzolan. Constr. Build. Mater. 36:305-310. https://doi.org/10.1016/j.conbuildmat.2012.04.011.
24. Chinchón-Payá S, Aguado A, Chinchón S. 2012. A comparative investigation of the degradation of pyrite and pyrrhotite under simulated laboratory conditions. Engineer. Geol. 127:75-80. https://doi.org/10.1016/j.enggeo.2011.12.003.
25. Salvador RP, Cavalaro SHP, Segura I, Figueiredo AD, Pérez J. 2016. Early age hydration of cement pastes with alkaline and alkali-free accelerators for sprayed concrete. Constr. Build. Mater. 111:386-398. https://doi.org/10.1016/j.conbuildmat.2016.02.101.
26. Teichmann G. 1990. The use of colorimetric methods in the concrete industry. Beton. Fertig.-Tech./Concr. Precast. Plant Technol. 10:58-73.
27. López A, Guzmán GA, Di Sarli AR. 2016. Colour stability in mortars and concretes. Part 1: Study on architectural mortars, Constr. Build. Mater. 120:617-622. https://doi.org/10.1016/j.conbuildmat.2016.05.133.
28. López A, Di Sarli AR. 2020. Measurements number in cementitious mixtures to define the colour and its homogeneity. Constr. Build. Mater. 238:117636. https://doi.org/10.1016/j.conbuildmat.2019.117636.
29. López A, Tobes JM, Giaccio G, Zerbino R. 2009. Advantages of mortar-based design for coloured self-compacting concrete. Cem. Concr. Compos. 31(10):754-761. https://doi.org/10.1016/j.cemconcomp.2009.07.005.
30. Afremow LC, Vanderberg JT. 1966. High resolution spectra of inorganic pigments and extenders in the mid-infrared region from 1500 cm^{-1} to 200 cm^{-1}. J. Paint. Technol. 38(495):169-202.
31. Sancho JP, Restrepo OJ, García P, Ayala J, Fernández B, Verdeja LF. 2008. Ultramarine blue from Asturian "hard" kaolins. Appl. Clay Sci. 41(3-4):133-142. https://doi.org/10.1016/j.clay.2007.10.005.
32. Landman A, de Waal D. 2004. Fly ash as a potential starting reagent for the synthesis of ultramarine blue. Mater. Res. Bull. 39(4-5):655-667. https://doi.org/10.1016/j.materresbull.2003.12.002.
33. Jakobsson S. 2002. Determination of Si/Al ratios in semicrystalline aluminosilicates by FT-IR spectroscopy. J. Appl. Spectros. 56(6):797-799. https://doi.org/10.1366/000370202760077559.